Hindawi
Complexity
Volume 2019, Article ID 3928268, 10 pages
https://doi.org/10.1155/2019/3928268

Research Article

A Decentralized Energy Flow Control Framework for Regional Energy Internet

Guofeng Wang, Kangli Zhao, Yu Yang, Junjie Lu, and Youbing Zhang

College of Information Engineering, Zhejiang University of Technology, Hangzhou 310023, China

Correspondence should be addressed to Youbing Zhang; zyoubing6858@sina.com

Received 26 July 2019; Accepted 17 September 2019; Published 28 October 2019

Guest Editor: Xiaoqing Bai

As a new form of smart grid, the energy transmission mode of the Energy Internet (EI) has changed from one direction to the interconnected form. Centralized scheduling of traditional power grids has the problems of low communication efficiency and low system resilience, which do not contribute to long-term development in the future. Owing to the fact that it is difficult to achieve an optimal operation for centralized control, we propose a decentralized energy flow control framework for regional Energy Internet. Through optimal scheduling of regional EI, large-scale utilization and sharing of distributed renewable energy can be realized, while taking into consideration the uncertainty of both demand side and supply side. Combing the multiagent system with noncooperative game theory, a novel electricity price mechanism is adopted to maximize the profit of the regional EI. We prove that Nash equilibrium of theoretical noncooperative game can realize consensus in the multiagent system. The numerical results of real-world traces show that the regional EI can better absorb the renewable energy under the optimized control strategy, which proves the feasibility and economy of the proposed decentralized energy flow control framework.

1. Introduction

The third industrial revolution is emerging, represented by new energy technologies and Internet technologies. Construction of Energy Internet (EI) can promote industrial technology upgrading and structural adjustment in modern energy industry [1, 2]. The concept of Energy Internet combines advanced power electronics technology, the Internet of Things (IoT) technology, and intelligent control technology. In EI, a large number of energy nodes, distributed energy harvesting devices, distributed energy storage devices, and various types of loads are interconnected to achieve energy multidirectional flowing and peer-to-peer energy sharing and trading.

As a subnetwork of Energy Internet, energy local network (ELN) has a variety of energy absorption methods. The ELN is a multienergy operation system, where different energy networks have strong coupling. The complementarity of energy can greatly improve the energy efficiency of the system to achieve cascade utilization of diverse energy sources [3–5]. On the contrary, the relationship between the demand side and the ELN is more flexible, which brings significant uncertainty to the operation and management in practice [6, 7]. The energy flow model of the heating network is established in [8], which explored the optimization of integrated energy system operation with a heat network. The northern part of Haidian District in Beijing was selected as a practical case in [9]. An optimal joint-dispatch scheme of energy and reserve is proposed in [10] for combined cooling, heating, and power (CCHP)-based MGs to effectively provide more reserve capability for the power system.

Due to the diversification of load patterns and stochastic nature of renewable energy sources in EI, the traditional centralized optimization scheduling method is difficult to apply in practice in actual operation. How to cope with the problem has become urgent to be solved in the management and optimization operation of EI [11, 12]. A hierarchical control architecture suitable for the energy management system of ELN is proposed, and a demonstration case of ELN energy management system a in [13]. The generalized "source-network-load-storage" of

the coordinated and optimized operation mode and public energy policy suggestion of ELN is proposed in [14]. The framework of hierarchical integration is designed to solve the problem of energy and information management for network connection in large-scale renewable energy source (RES) in [15]. However, the above research focuses on the architecture of operation, which neglects the impact of individuality and the flexibility of conversion in the regional EI. The overall description of the multi-ELN systems structure and the extraction of typical characteristics are missing, so the feasibility has been limited in practice.

Motivated by the above facts, we analyze the operation pattern of energy flow in a typical architecture of the ELN framework in order to obtain the optimal operation of multienergy. A strategy of optimal operation in EI is proposed based on the multiagent system (MAS) combined with noncooperative game theory to realize the decentralized control of the ELN system. The real-time electricity price is obtained by iterative optimization, which maximizes the overall profit of the EI system. For each ELN, a quadratic programming problem is developed with the aim to increase the individual economic benefit. Through energy trading and conversion between ELNs, the balance of supply side and demand side of the overall EI system is enhanced. As a result, the resilience and economy of the EI system are significantly enhanced.

The remainder of the paper is organized as the following. In Section 2, the typical architecture of ELN is demonstrated and the basic models in ELN are provided. An optimal energy flow control framework based on the multiagent system and the novel electricity price in the ELN is proposed in Section 3. Simulation results and conclusions are provided in Sections 4 and 5, respectively.

2. Multi-ELN System Configuration

2.1. The Architecture of ELN. ELN is a collection of a complete future-oriented energy system constructed from the aspects of energy production, transmission, distribution, transformation, and consumption. It is a power-centric interactive and shared platform for all kinds of energy which enables smart mutual supply of different types of loads. Figure 1 shows a typical architecture for ELN constructed in this paper. The system of ELN includes primary energy, energy conversion devices, energy storage devices, and intelligent load. Primary energy can meet the side of the electrical/thermal/cooling load requirements through the energy conversion device. Through the correlation and complementarity of multiple energy systems in discrete-time scales, multienergy cascade utilization can be realized, which enables load peak transferring. Carbon emission can be significantly reduced by increasing the utilization rate of RES.

The EI consists of ELNs, which are highly coupled products of multiple type energy and information networks. With huge number of diverse energy equipment in EI, centralized control cannot deal with the rapidly increasing data complexity, and it is difficult to make full use of the energy in EI. As a result, the stability and economy of the power system will be impacted. Based on the aforementioned, we propose a decentralized energy flow control framework of multiagent EI to effectively improve computing and execution of system operating.

A discrete-time model is considered in this paper. Assume that the optimal range (e.g., 24 h) is divided into T discrete periods with an interval of Δt, which is denoted by t.

2.2. Basic Model in ELN. As the basic scheduling unit in EI, the energy storage system (ESS) can compensate for the power difference caused by the volatility of the RESs and the load. The model of the ESS can be described as follows:

$$I_i = \left[S_i^0, S_i^{\mathrm{E}}, Q_i^{\max}, P_i^{\mathrm{c}}, P_i^{\mathrm{d}}\right], \tag{1}$$

where S_i^0 represents the initial state of charge in the energy storage system; S_i^{E} represents the expected capacity of the energy storage system; $Q_i^{\max}$ represents the rated capacity of ESS; and P_i^{c} and P_i^{d} represent the charging/discharging power of i ESS, respectively.

We assumed that all energy storage systems have the same lithium-ion battery pack and the charging/discharging power over a single period of time is considered constant [16]. Therefore, the model and constraints of the energy storage system battery are established as follows:

$$\begin{cases} S_i^{t+1} = M_i S_i^t + B_i P_i^t, \\ Y_i^t = C_i S_i^t + D_i P_i^t, \end{cases} \tag{2}$$

where S_i^{t+1} and S_i^t represent the state of SOC at period $t+1$ and t, respectively; Y_i^t represents the output of PEV i at period t; M_i, B_i, C_i, and D_i represent the system matrix, input matrix, output matrix, and feed-forward matrix, respectively; and P_i^t represents the power of SOC at period t, which can be denoted as

$$\begin{gathered} P_i^t = \left[P_{\mathrm{ch},i}^t, P_{\mathrm{dch},i}^t\right]^{\mathrm{T}}, \\ \left(M_i, B_i, C_i, D_i\right) = \left(1, \frac{\Delta t}{Q_i^{\max}}\left[\eta_{\mathrm{ch}} - \frac{1}{\eta_{\mathrm{dch}}}\right], 0, [1-1]\right), \end{gathered} \tag{3}$$

where $P_{\mathrm{ch},i}^t$ and $P_{\mathrm{dch},i}^t$ represent the charging/discharging power of the energy storage system at period t, respectively, and η_{ch} and η_{dch} represent the charging/discharging efficiency, respectively.

Since the SOC at period t are bounded by the rated capacity of ESS, we have

$$Q_i^{\min} \le S_i^t \le Q_i^{\max}, \tag{4}$$

where $Q_i^{\min}$ and $Q_i^{\max}$ denote the minimum and maximum capacity of ESS, respectively.

2.3. Gas Turbine Model. Gas turbine is a vital device for EI with high efficiency, which can fully utilize natural gas energy and contribute to reducing environmental pollution. The output of the gas turbine is expressed as follows:

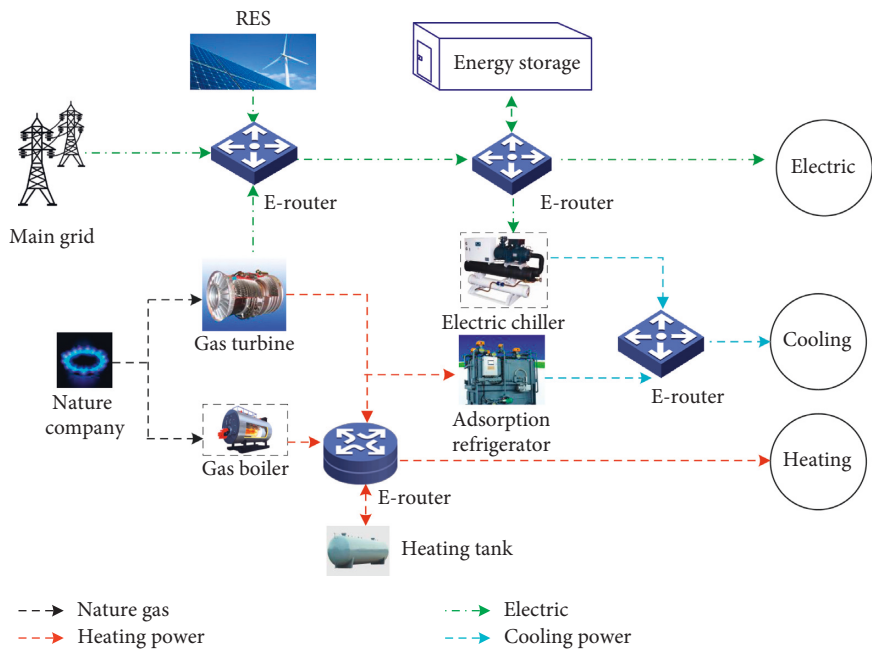

Figure 1: The typical architecture of ELN framework.

$$P^t_{\mathrm{GT},i} = \eta_c \lambda_{\mathrm{gas}} \gamma_{\mathrm{gt}},$$
$$Q^t_{\mathrm{r},i} = \frac{P^t_{\mathrm{GT},i}\eta_{\mathrm{r}}}{\eta_{\mathrm{c}}}, \tag{5}$$
$$0 \le P^t_{\mathrm{GT},i} \le P^{\max}_{\mathrm{GT},i},$$

where $P^t_{\mathrm{GT},i}$ represents power generation of the gas turbine in i ELN at t period; $P^{\max}_{\mathrm{GT},i}$ represents maximum power generation of gas turbines; $Q^t_{\mathrm{r},i}$ represents waste heat recovery power of the gas turbine in i ELN at t period; η_{c} and η_{r} represent power generation efficiency and waste heat recovery efficiency for gas turbines, respectively; γ_{gt} represents the gas consumption rate; and λ_{gas} represents the calorific value of natural gas.

The active power output of the gas turbine is bounded by the ramping constraints, denoted as

$$\begin{cases} P^{t+1}_{\mathrm{GT},i} - P^t_{\mathrm{GT},i} \le P^{\mathrm{Up}}_{\mathrm{GT},i}, \\ P^t_{\mathrm{GT},i} - P^{t+1}_{\mathrm{GT},i} \le P^{\mathrm{Down}}_{\mathrm{GT},i}, \end{cases} \tag{6}$$

where $P^{\mathrm{Up}}_{\mathrm{GT},i}$ and $P^{\mathrm{Down}}_{\mathrm{GT},i}$ represent the ramp-up power and ramp-down power constraints, respectively.

2.4. Cold/Heat Load Model. The gas turbine waste heat is mainly recycled by heat exchangers and adsorption refrigerators for refrigeration. Specific physical modeling is shown as follows:

(1) Heat exchanger:

$$P^t_{\mathrm{HX},i} = Q^t_{\mathrm{HX},i}\eta_{\mathrm{HX}}, \tag{7}$$

where $P^t_{\mathrm{HX},i}$ represents the output heat power of the heat exchanger; $Q^t_{\mathrm{HX},i}$ represents the heat absorbed by the heat exchanger from the gas turbine; and η_{HX} represents heat exchange efficiency of the heat exchanger.

(2) Adsorption refrigerator:

$$P^t_{\mathrm{AR},i} = Q^t_{\mathrm{AR},i}\eta_{AR}, \tag{8}$$

where $P^t_{\mathrm{AR},i}$ represents the output cooling power of the adsorption refrigerator; $Q^t_{\mathrm{AR},i}$ represents the heat absorbed by an adsorption refrigerator from a gas turbine; and η_{AR} represents the refrigeration efficiency of the adsorption refrigeration machine. The total absorption heat power of heat exchange gas and adsorption refrigerators should meet the following requirements:

$$Q^t_{\mathrm{AR},i} + Q^t_{\mathrm{HX},i} \le Q^t_{r,i}. \tag{9}$$

(3) Gas boiler:

When the thermal power of the system is insufficient, it is supplemented by the heat generated by the gas-fired boiler. The output thermal power of the gas-fired boiler is expressed as follows:

$$F_{\mathrm{GB},i} = \frac{\sum_{t=1}^{T} P^t_{\mathrm{GB},i}}{\eta_{\mathrm{GB}}\lambda_{\mathrm{gas}}},$$
$$0 \le P^t_{\mathrm{GB},i} \le P^{\max}_{\mathrm{GB},i}, \tag{10}$$

where $P^t_{\mathrm{GB},i}$ represents the thermal power of gas fired boilers; $F_{\mathrm{GB},i}$ is the amount of natural gas consumed by gas fired boilers at $[t, T]$ period; $P^{\max}_{\mathrm{GB},i}$ represents the maximum output heat power of gas fired boilers; and η_{GB} represents the operating efficiency of gas fired boilers.

2.5. Uncertainty Analysis. The scenario in power grid is a kind of operation state of the power system [17]. The scene reduction is to eliminate the unrepresentative or error scenes and retain the typical scenes, without affecting the accuracy of the evaluation. We use the reduction method of typical scenes to characterize the uncertainty of load and output of renewable generation [18]. Multiple scenes are simulated by Monte Carlo method, based on the prediction of wind speed and solar radiation angle. Random scenes are generated by the method of distributed sampling which simulates fluctuations in predicted values under actual conditions.

The random distribution error is obtained by the forecasting error and its probability distribution which is determined based on historical data. The random variable of RES is converted to output power based on the output characteristic curve. In this paper, the predicted value of RES output at period T in the future is expressed as time series based on the method of backward reduction. The scenario of output is assumed as $\omega_i = (\lambda_i^0, \lambda_i^1, \ldots, \lambda_i^t, \lambda_i^T)$, where λ_i^t represents the value of scene i at period t; the corresponding probability of occurrence of scene ω_i is P_i; and the minimum probability distance between the scene set reduction and the final reserved scene subset is expressed as follows:

$$\mathrm{Min}\sum_{i\in\alpha} p_i \times \min_{j\notin\alpha} d\left(\omega_i, \omega_j\right), \tag{11}$$

where α represents the scene collection which is eventually deleted; the total number of scenes is set as 3000. The reserved set $S = \{\omega_0, \omega_1, \omega_i, \omega_s\}$ is initialized. We add another scene with the smallest distance of probability in the actual reduction set. The probability of the scene ω_l closest to the reduced set is changed to $p(\omega_l') = p(\omega_l) + p(\theta_k)$, until the number of scenes contained in the reduction set meets the requirements.

RES system operates in the Maximum Power Point Tracking (MPPT) mode which can adapt to environmental changes in real time to achieve maximum output [19]. Based on the short-time prediction results, the active power of RES output and basic load is shown as

$$\begin{aligned} P_{\mathrm{PV},i} &= \left[P_{\mathrm{PV},i}^1, P_{\mathrm{PV},i}^2, \ldots, P_{\mathrm{PV},i}^{\mathrm{T}}\right], \quad i \in [1, 2, \ldots, n], \\ P_{\mathrm{WT},i} &= \left[P_{\mathrm{WT},i}^1, P_{\mathrm{WT},i}^2, \ldots, P_{\mathrm{WT},i}^{\mathrm{T}}\right], \quad i \in [1, 2, \ldots, n], \\ P_{\mathrm{Load},i} &= \left[P_{\mathrm{Load},i}^1, P_{\mathrm{Load},i}^2, \ldots, P_{\mathrm{Load},i}^{\mathrm{T}}\right], \quad i \in [1, 2, \ldots, n]. \end{aligned} \tag{12}$$

The total power of RES output in this paper is

$$P_{\mathrm{RES},i} = P_{\mathrm{PV},i} + P_{\mathrm{WT},i}. \tag{13}$$

According to the components of the power supply side and the demand side in the ELN, the power balance model can be obtained:

$$\begin{aligned} P_{\mathrm{RES},i}^t + P_{\mathrm{GT},i}^t - P_{\mathrm{Load},i}^t - P_{\mathrm{dch},i}^t - P_{\mathrm{EC},i}^t &= u_{\mathrm{grid},i}^t + P_{\mathrm{ch},i}^t, \\ u_{\mathrm{grid},i}^t &\le u_{\mathrm{grid},i}^{\max}, \end{aligned} \tag{14}$$

where $u_{\mathrm{grid},i}^t$ represents the interaction power between i ELN and the EI system; $P_{\mathrm{EC},i}^t$ represents the electric refrigerator power which provides cold load for the system; and $u_{\mathrm{grid},i}^{\max}$ represents the power constraint of timeline.

3. A Decentralized Energy Flow Control Framework

3.1. The Construction of MAS in EI. Multiagent is a network structure composed of agents with the characteristics of autonomy, decentralized control, and bidirectional communication with other agents [20, 21]. Autonomous and intelligent systems have been widely used in energy systems. The centralized control cannot handle a variety of global information. Each agent in the multiagent system (MAS) could collect its own environmental information to solve the optimization problems and reach global consensus eventually in the autonomous region EI [22]. Considering the different characteristics and functions of nodes, the types of agents can be classified into the following:

(1) Intelligent measurement agent (IMA): it monitors and reports the operation status, power output status, and load demand status of internal equipment in the ELN system, which is responsible for the monitoring for the balance of the supply side and the demand side.

(2) Scheduling management agent (SMA): according to the information uploaded by the IMA and electricity price agent (EPA), the internal equipment output optimization is executed. When there is a shortage or excess load, the information is reported to the EPA for further addressing.

(3) Electricity price agent (EPA): it receives information of each ELN by the IMA and SMA. According to the real-time supply-demand balance of the system, the global optimal equilibrium solution is calculated. As the most essential agent, the strategy of maximizing EI benefits is the consensus reached by all EPAs in decentralized decision-making [23].

3.2. The Mechanism of Electricity Price. Different from the previous method of static electricity price that determines its own electricity price by the power grid [24], we adopt a new mechanism of electricity price. The electricity price in the EI is obtained based on the competition between ELN and the consensus reached by the MAS.

Since multiple energy sources can be converted into electricity, we use electricity as the core of trading in the energy flow control mechanism. In the electricity market of EI, the agent of electricity price takes part in the bidding to maximize the benefit of ELN.

The key problem is to obtain the optimal electricity price which maximizes the profit of ELN:

$$P = \sum_{t=1}^{\tau}\left[\left(\hat{r}_{\mathrm{b}} - r_{\mathrm{b}}\right)^2 + \left(\hat{r}_{\mathrm{s}} - r_{\mathrm{s}}\right)^2\right] + \lambda_n \times \sum_{t=1}^{\tau}\left[\left(r_{\mathrm{b}} - a_1^t\right)^2 + \left(r_{\mathrm{b}} - a_2^t\right)^2\right], \tag{15}$$

$$a_1^t = \begin{cases} \dfrac{m_1^t}{c_1^t}, & c_1^t \neq 0, \\ \lambda_{\mathrm{b}}, & c_1^t = 0, \end{cases} \qquad a_2^t = \begin{cases} \dfrac{m_2^t}{c_2^t}, & c_2^t \neq 0, \\ \lambda_{\mathrm{s}}, & c_2^t = 0, \end{cases} \tag{16}$$

where P represents the optimization goal of the electricity price agent in the rolling time periods; λ_n represents a flexible constraint coefficient of electricity price variables; r_{b} and r_{s} represent the internal purchasing price and internal selling price of electricity during the day, respectively; λ_{b} and λ_{s} represent the initial values of the internal purchasing price and internal selling price of electricity during the day, respectively; $\hat{r}_{\mathrm{b}}$ and $\hat{r}_{\mathrm{s}}$ represent the day-ahead internal purchase price and internal sale price; and a_1^t and a_2^t represent the reference price of power balance, which correspond to the electricity price in power selling and purchasing when the net load is zero, respectively. In addition, the expressions of the four variables c_1^t, c_2^t, m_1^t, and m_2^t are as follows:

$$\begin{cases} c_1^t = \displaystyle\sum_{i\in \mathrm{B}}\left(u_{\mathrm{grid},i}^t + \frac{P_{\mathrm{Load},i}^{\mathrm{E},t}\lambda_{\mathrm{b}}}{r_{\mathrm{b}}}\right), \\ c_2^t = \displaystyle\sum_{i\in \mathrm{S}}\left(u_{\mathrm{grid},i}^t + \frac{P_{\mathrm{Load},i}^{\mathrm{E},t}\lambda_{\mathrm{s}}}{r_{\mathrm{s}}}\right), \\ m_1^t = \displaystyle\sum_{i\in \mathrm{B}}\left(P_{\mathrm{Load},i}^{\mathrm{E},t}\lambda_{\mathrm{b}}\right), \\ m_2^t = \displaystyle\sum_{i\in \mathrm{S}}\left(P_{\mathrm{Load},i}^{\mathrm{E},t}\lambda_{\mathrm{s}}\right), \end{cases} \tag{17}$$

where $P_{\mathrm{Load},i}^{\mathrm{E},t}$ represents the basic load in i ELN and $u_{\mathrm{grid},i}^t$ represents the interactive power between the i ELN and EI.

3.3. Components of Game Theoretic Model. The mixed integer model is established by the problem of optimization in optimization periods; the following are the detailed components of the game model.

3.3.1. Players. The players are all the agents of electricity price in the set N^+ which includes RES and the battery energy storage system (BESS).

3.3.2. Game Rules

(i) Action: for any $i \in N^+$ in the k period, $A_i^k = \{P \mid \text{Constraints}\,(14) - (17)\}$ is the collection of all players' action.

(ii) Information: it includes RESs and various demand load and strategies adopted by other players.

(iii) Strategies: each participant's revenue is maximized by an optimized strategy, which can be expressed as a feasible strategy set ρ_i, shown as follows:

$$\rho_i = \{J \mid \text{Constraints}\,(1) - (3), (14) - (17)\}. \tag{18}$$

3.3.3. Payoffs. It is used to measure the benefit of the players in the game; the payoff of each player is maximized, expressed as U_i:

$$U_i = \left\{J + P \times U_{\mathrm{grid}} \mid \text{Constraints}\,(1) - (3), (13) - (17)\right\}. \tag{19}$$

Based on the above set of strategy, $A_i = \{A_1, A_2, \ldots, A_N\}$ if and only if the following conditions are satisfied:

$$U_i\left(A^*\right) \geq U_i\left(A\right), \quad \forall P \in A_i, \forall i \in N^+, \tag{20}$$

where A^* represents the set after updating the policy set, and the policy vector A^* is called Nash equilibrium, where no regional ELN can improve the respective benefits by unilaterally changing the strategy [25].

The strategy P_i is the interaction price of i ELN; the energy price strategy of the i ELN is A_i; $P_{\max}$ is the maximum value of the exchangeable electricity price; and A_i is a compact convex subset, while the participants sell power during the game. The electrical strategy P exists; therefore, the set A_i is not empty.

Prove that $U_i\left(A\right)$ is a concave function; then, S has a pure strategy Nash equilibrium point. For the second derivation, the second derivative is as follows:

$$\frac{\partial^2 U}{\partial a_i^2} = 2 - 4\lambda_n \times \left[\frac{2P_{\mathrm{Load},i_1}\lambda_{\mathrm{b}} r_{\mathrm{b}}^3}{\left(u_{\mathrm{grid},i_1} r_{\mathrm{b}} + P_{\mathrm{Load},i_1}\lambda_{\mathrm{b}} r_{\mathrm{b}}\right)^4} + \frac{2P_{\mathrm{Load},i_2}\lambda_{\mathrm{b}} r_{\mathrm{b}}^3}{\left(u_{\mathrm{grid},i_2} r_{\mathrm{b}} + P_{\mathrm{Load},i_2}\lambda_{\mathrm{b}} r_{\mathrm{b}}\right)^4}\right]. \tag{21}$$

Since $r_{\mathrm{b}}, \lambda_{\mathrm{b}}, P_{\mathrm{Load},i_1}$ $(i = 1, 2, 3, \ldots, N)$ is nonnegative, that is, $(\partial^2 U/\partial a_i^2) < 0$, U_i is strictly concave [26]. In summary, the automated demand response game is a typical strictly concave N-person game [27, 28]; therefore, the existence and uniqueness of the NE is proved.

3.4. Daily Cost Model of ELNs. In the game model, each agent can know others strategies in each round of decision-making [29]. Based on the short-term load forecasting data, the decision variables are optimized and updated. The optimization goal of this paper is to minimize the total operating cost of a single ELN. The optimization problem of a single

```
Initialization: P_PV, P_WT, P_Load, and each EPA.
Transmit initial strategy according to players' requirements to its neighbors.
A new iteration starts when the strategy information is updated.
   Real-time optimization
for i = 1 do
   for k = 1 : 48 do
      Input predicted value of P_PV, P_WT, and P_Load.
      Update P and J_i based on (15) and (22).
      while there is no further improvement do
         k = k + 1.
      end while
   end for
   if the optimized scheduling is different from the previous scheduling strategy then
      Send the new strategy to the MAS.
   else
      Denied, retain the previous control strategy.
   end if
end for
```

Algorithm 1: Decentralized energy flow control strategy.

ELN in the rolling time domain can be expressed as a quadratic programming problem:

$$\begin{aligned} J_i = & \sum_{i=1}^{M}\sum_{i=1}^{\tau}\left(\widehat{u}_{\text{grid},i}^{t} - u_{\text{grid},i}^{t}\right)^2 \\ & + A \times \sum_{i=1}^{\tau}\left(\widehat{Q}_{\text{s},i}^{t} - Q_{\text{s},i}^{t}\right)^2 + B \times \sum_{i=1}^{\tau}\left(\widehat{P}_{\text{GT},i}^{t} - P_{\text{GT},i}^{t}\right)^2 \\ & + C \times \sum_{i=1}^{\tau}\left(\widehat{Q}_{\text{HX},i}^{t} - Q_{\text{HX},i}^{t}\right)^2 + D \times \sum_{i=1}^{\tau}\left(\widehat{Q}_{\text{AR},i}^{t} - Q_{\text{AR},i}^{t}\right)^2 \\ \text{s.t.} \quad & (2)-(10),\ (13)-(17), \end{aligned} \tag{22}$$

where J_i represents the time domain length in optimized scrolling; $\widehat{u}_{\text{grid},i}^{t}$ and $u_{\text{grid},i}^{t}$ represent the day-ahead and the real-time energy interaction power, respectively; $\widehat{Q}_{\text{s},i}^{t}$ and $Q_{\text{s},i}^{t}$ represent the day-ahead and real-time remaining capacity of ESS, respectively. $\widehat{P}_{\text{GT},i}^{t}$ and $P_{\text{GT},i}^{t}$ represent the day-ahead and real-time power generation of the gas turbine, respectively; $\widehat{Q}_{\text{HX},i}^{t}$ and $Q_{\text{HX},i}^{t}$ represent the day-ahead and real-time waste heat of the gas turbine for heating, respectively; $\widehat{Q}_{\text{AR},i}^{t}$ and $Q_{\text{AR},i}^{t}$ represent the day-ahead and real-time waste heat of the gas turbine for refrigeration, respectively; and A, B, C, and D represent the flexible constraint coefficient corresponding to the four components, respectively.

3.5. Solution Process. According to the aforementioned models, the proposed decentralized energy flow control strategy will be used to determine the regional ELN scheduling plan, which is shown in Algorithm 1.

4. Case Studies

To verify the validity of the proposed energy flow control strategy, four typical ELNs with different structures are chosen for case analysis [30]. The power supply side of each ELN consists of PV, WT, gas turbine, ESS, and the main grid; and the demand side is equipped with basic loads and electric refrigerators. Among them, energy interaction between the ELN is completed by a single bus, and the energy net payload is interacted with the external power grid through a single bus after the interaction. The parameters of rated power of PV output, WT output, BESS capacity, and gas turbine capacity of each ELN system are shown in Table 1. The ELN bus power transmission capacity is set to 4000 kW, and the maximum charging and discharging power of ESS is set to 2000 kW. In addition, the parameters associated with the energy conversion equipment are provided in Table 2.

The output power of RESs is given in Figure 2, which shows the output power of PV and WT of four ELNs in a typical day, respectively. Output power of cooling/heating load is shown in Figure 3.

In order to precisely quantify the optimization effect of the proposed energy flow control strategy, in this section, we simulate the following three models simultaneously in the EI. The three cases are demonstrated as follows:

Case I. No optimization mode is implemented. The power generation equipment is running at full capacity in an ELN, with no power interactions with other ELNs.

Case II. Each ELN performs power interactions without further optimization.

Case III. The proposed energy flow control strategy based on noncooperative game with MAS.

Analyze and compare the energy net load characteristics and economy of the three operating modes. The load curve of the three cases is depicted in Figure 4.

As shown in Figure 4, compared with Case I and Case II, Case III is decreased by 82.44% and 29.22% in terms of peak-to-valley difference, respectively. The volatility is reduced by 80.05% and 27.08%, respectively. The proposed energy flow control strategy can effectively reduce the power difference

Table 1: The basic parameters of ELN.

Types	PV (kW)	WT (kW)	BESS (kWh)	Gas turbine (kW)
ELN 1	3000	2500	13000	2000
ELN 2	3300	3550	13000	2000
ELN 3	4000	3900	13000	1000
ELN 4	3500	3750	13000	1000

Table 2: The parameters of energy conversion equipment.

Types	Heat exchanger (kW)	Absorption chiller (kW)	Gas boiler (kW)	Electric refrigerator (kW)
ELN 1	2000	2000	1500	1000
ELN 2	2000	0	1500	0
ELN 3	0	2000	0	1000
ELN 4	0	0	0	0

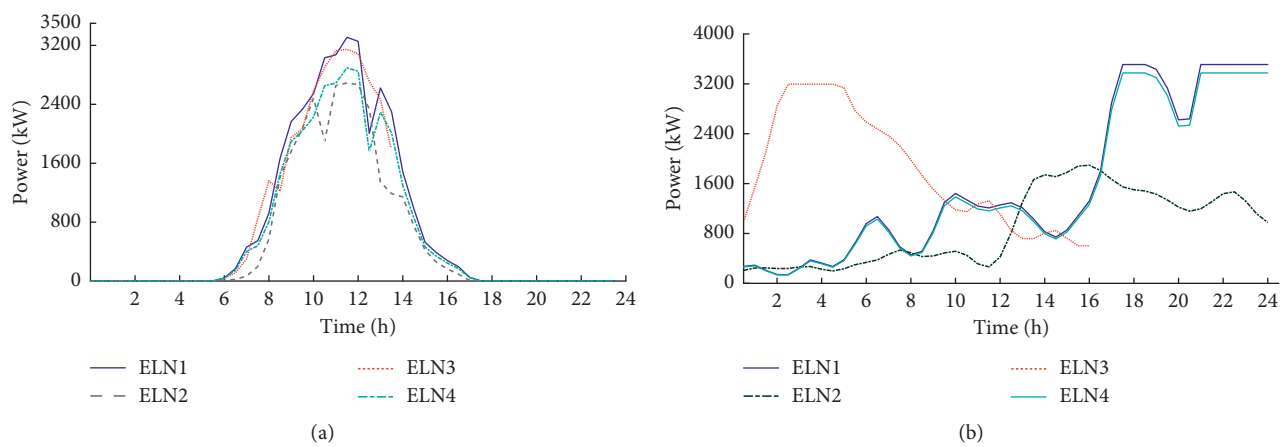

Figure 2: Active power of PV and WT output in a typical day.

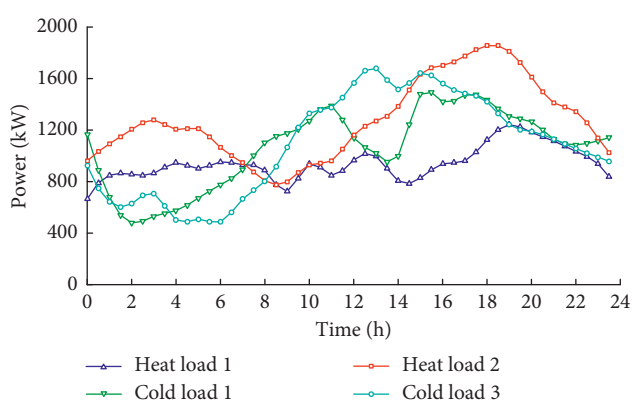

Figure 3: The cooling and heating loads of ELNs.

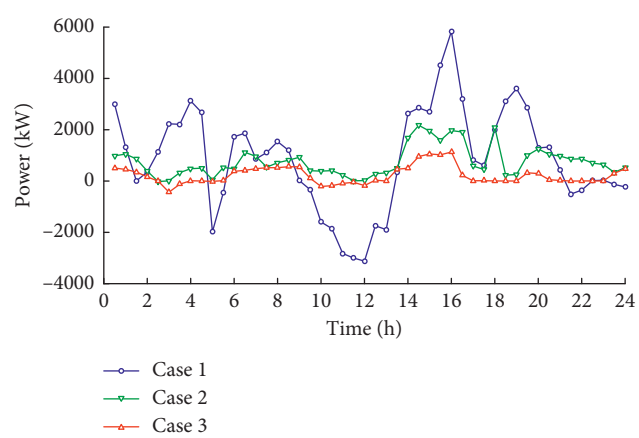

Figure 4: The net load of the Energy Internet under three cases.

existing in the EI and improve the stability and resilience of the system. In addition, compared with Case I, the energy utilize efficiency in the other two cases has significantly improved.

It can be observed from Figure 5, when the output power of RESs is insufficient, the ESS and gas turbine is operated. Each ELN actively conducts power interactions to stabilize system load fluctuations, where the ESS and gas turbine play a vital role in outputting power. When the gas turbine output is in deficit, the waste heat utilization is also insufficient. At this time, the heat load is mainly provided by the gas boiler, while the cooling load is mainly provided by the electric refrigerator. When the gas turbine output is surplus, the heat load is mainly provided by the gas turbine and the remaining heat is fully utilized. In addition, refrigeration can meet the demand

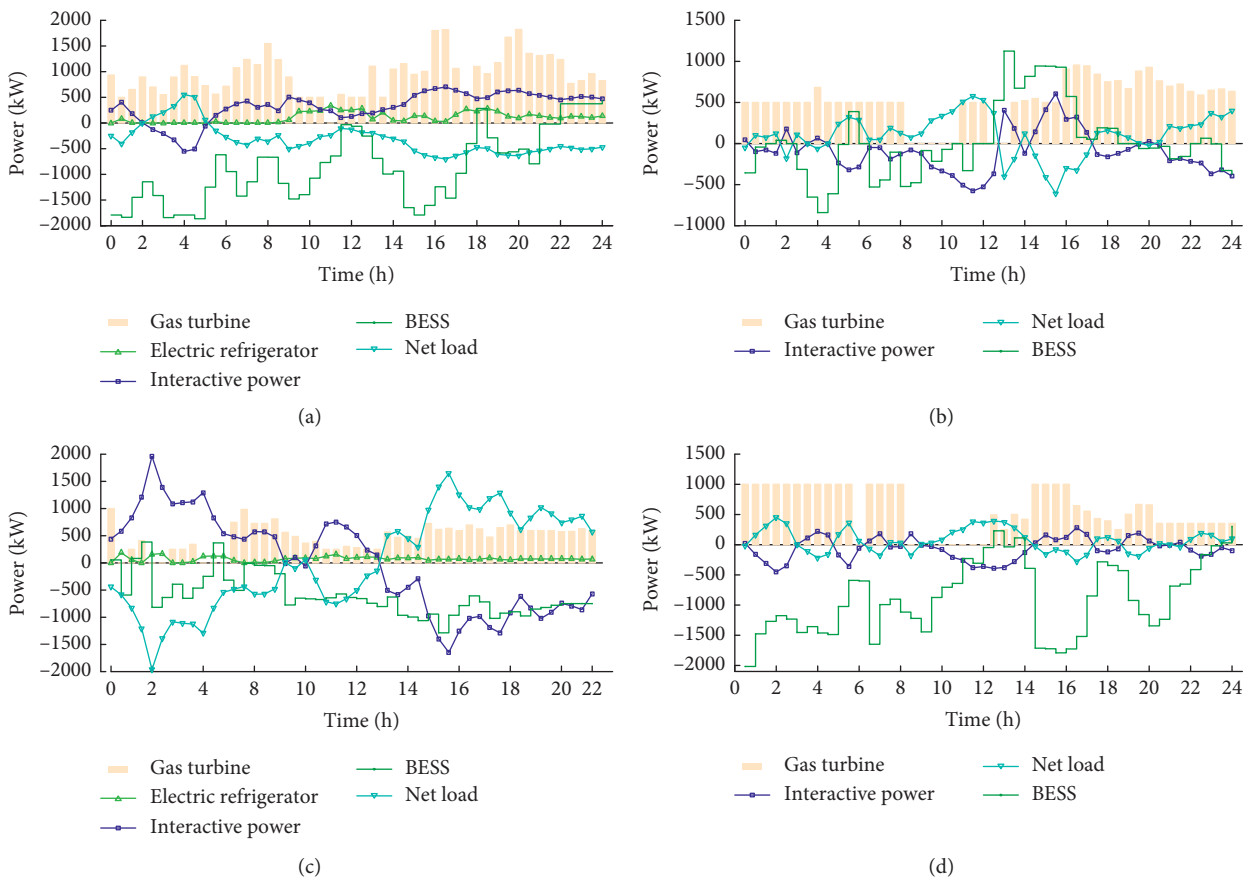

Figure 5: Optimal scheduling results of four ELNs.

for cold load. As a result, the overall operating efficiency and fuel utilization of the EI system are significantly improved.

The detailed comparison of time-of-use pricing and real-time pricing obtained by the proposed game theoretic model as mentioned above is illustrated in Figure 6. Time-of-use electricity prices cannot demonstrate the internal energy difference, which has a negative effect on energy interaction. According to the internal energy consumption of each ELN, the ultimate interaction price is determined through mutual game process. After multiple iterations, the electricity price tends to be stable. All participants choose not to change their strategies and maximize their respective interests. Each participant in the EI network price gets the optimal strategy through the game, repeating this convergence process, and finally realizes the consensus that no ELN can obtain more profit.

Table 3 presents the detailed results of various costs in three cases.

(1) Comparing Case II and Case III with Case I, the RES utilization rate has been significantly improved, when the abandoned RES power loss is close to 0. The photoelectric subsidy has increased by 4.85% and 4.82%, respectively. In addition, Case 3 has a slight increase in charging/discharging loss, power loss, and operation and maintenance costs compared with Case II, indicating that the optimization process has little influence on the economy with less transaction cost.

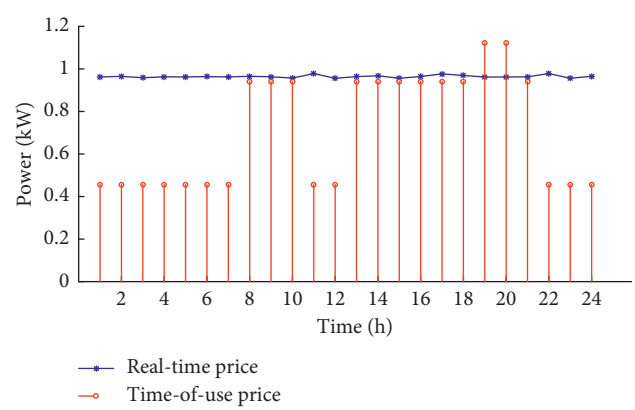

Figure 6: Comparison of two types of electricity price.

(2) Compared with Case I and Case II, Case III has increased the total revenue by 290.06% and 123.31%, respectively, indicating that the game-theoretical decentralized optimization process can significantly improve the economics of EI. It is obvious that the overall benefit is significantly increased by fully utilizing the output of RES with real-time electricity price mechanism.

(3) Compared with Case I, natural gas costs of Case II and Case III have increased by 11.01% and 4.52%,

Table 3: Economic statistics of three cases.

Types	Case I	Case II	Case III
Loss cost of RES abandoning (yuan)	2240.5	0	17.5
Transaction cost of power grid (yuan)	25991.7	17172.2	4804. 4
Charging and discharging loss (yuan)	0	1129.6	1173.2
Photoelectric subsidy (yuan)	77532.6	81296.6	81267.2
Operational and maintenance cost	6268.2	6587.6	6662.9
Gas cost (yuan)	66357.5	73663.3	69358.9
Multienergy supply income (yuan)	31453.4	31453.4	31453.4
Power loss (yuan)	0	2233.2	2319.5
Generation cost of gas turbine (yuan/kWh)	0.3243	0.3889	0.3733
Total revenue (yuan)	8128	14197.3	31703.8

respectively. The average power generation cost of gas turbines has increased by 19.92% and 15.11%, respectively, indicating that Cases II and Case III can transform heating and cooling power in more effective ways. Comparing Case III with Case II, it can be observed that the increase in natural gas costs is less which indicates that multienergy can actively participate in system optimization to reduce gas turbine output. The utilization of RES has also greatly improved the economic and environmental performance of the EI system.

5. Conclusion

In this paper, a decentralized energy flow control framework of optimal operation considering the uncertainty of the supply side and demand side has been proposed for the Energy Internet. A typical architecture of ELN is established with system models which can better reflect the characteristics and requirements of EI. In addition, a novel electricity price mechanism for energy interaction is proposed to respond to the supply-demand difference. The theoretical noncooperative game is proposed with the objective to minimize the daily operational cost of the EI system. Through iterative calculation, the game reaches the Nash equilibrium, which is the consensus reached by the MAS. The case study based on real-world data proves the feasibility and effectiveness of the proposed framework. The proposed decentralized framework combining with optimized operational strategy can contribute to reducing the system load volatility and decreasing the operating economic cost as well as improving the reliability and resilience of the EI system.

Data Availability

The data used to support the findings of this study are included within the article.

Conflicts of Interest

The authors declare no conflicts of interest.

Acknowledgments

This work was supported by the National Natural Science Foundation of China under grant 51777193.

References

[1] D. Cheng, "Controllability of switched bilinear systems," *IEEE Transactions on Automatic Control*, vol. 50, no. 4, pp. 511–515, 2005.

[2] A. Q. Huang, M. L. Crow, G. T. Heydt, J. P. Zheng, and S. J. Dale, "The future renewable electric energy delivery and management (FREEDM) system: the energy internet," *Proceedings of the IEEE*, vol. 99, no. 1, pp. 133–148, 2011.

[3] L. Ju, Z. Tan, H. Li, Q. Tan, X. Yu, and X. Song, "Multi-objective operation optimization and evaluation model for CCHP and renewable energy based hybrid energy system driven by distributed energy resources in China," *Energy*, vol. 111, pp. 322–340, 2016.

[4] S. Rech and A. Lazzaretto, "Smart rules and thermal, electric and hydro storages for the optimum operation of a renewable energy system," *Energy*, vol. 147, pp. 742–756, 2018.

[5] Q. Sun, R. Han, H. Zhang, J. Zhou, and J. M. Guerrero, "A multiagent-based consensus algorithm for distributed coordinated control of distributed generators in the energy internet," *IEEE Transactions on Smart Grid*, vol. 6, no. 6, pp. 3006–3019, 2015.

[6] N. Ahmed, M. Levorato, and G. P. Li, "Residential consumer-centric demand side management," *IEEE Transactions on Smart Grid*, vol. 9, no. 5, pp. 4513–4524, 2018.

[7] J. Wang, N. E. Redondo, and F. D. Galiana, "Demand-side reserve offers in joint energy/reserve electricity markets," *IEEE Transactions on Power Systems*, vol. 18, no. 4, pp. 1300–1306, 2003.

[8] G. U. Wei, L. U. Shuai, J. Wang, X. Yin, C. Zhang, and Z. Wang, "Modeling of the heating network for multi-district integrated energy system and its operation optimization," *Proceedings of the CSEE*, vol. 37, no. 5, pp. 1305–1316, 2017.

[9] C. Lin, L. Chen, S. Zhu, T. Hao, and X. Shen, "Study of micro energy internet based on multi-energy interconnected strategy," *Power System Technology*, vol. 40, no. 1, 2016.

[10] J. Wang, H. Zhong, Q. Xia, C. Kang, and E. Du, "Optimal joint-dispatch of energy and reserve for CCHP-based microgrids," *IET Generation, Transmission & Distribution*, vol. 11, no. 3, pp. 785–794, 2017.

[11] H. Ren, W. Zhou, K. i. Nakagami, W. Gao, and Q. Wu, "Multi-objective optimization for the operation of distributed energy systems considering economic and environmental aspects," *Applied Energy*, vol. 87, no. 12, pp. 3642–3651, 2010.

[12] Z. Huang, H. Yu, X. Chu, and Z. Peng, "A novel optimization model based on game tree for multi-energy conversion systems," *Energy*, vol. 150, no. 12, pp. 109–121, 2018.

[13] R. Lu, S. H. Hong, and X. Zhang, "A dynamic pricing demand response algorithm for smart grid: reinforcement learning approach," *Applied Energy*, vol. 220, pp. 220–230, 2018.

[14] M. Zeng, Y. Yang, D. Liu et al., ""Generation-grid-load-storage" coordinative optimal operation mode of energy internet and key technologies," *Power System Technology*, vol. 40, pp. 114–124, 2016.

[15] K. Wang, Y. Wang, Y. Sun, S. Guo, and J. Wu, "Green industrial internet of things architecture: an energy-efficient perspective," *IEEE Communications Magazine*, vol. 54, no. 12, pp. 48–54, 2016.

[16] C. Wei, M. Benosman, and T. Kim, "Online parameter identification for state of power prediction of lithium-ion batteries in electric vehicles using extremum seeking," *International Journal of Control, Automation and System*, pp. 1–11, 2019.

[17] P. Meibom, R. Barth, B. Hasche, H. Brand, C. Weber, and M. O'Malley, "Stochastic optimization model to study the operational impacts of high wind penetrations in Ireland," *IEEE Transactions on Power Systems*, vol. 26, no. 3, pp. 1367–1379, 2011.

[18] K. Mason, J. Duggan, and E. Howley, "Forecasting energy demand, wind generation and carbon dioxide emissions in Ireland using evolutionary neural networks," *Energy*, vol. 155, pp. 705–720, 2018.

[19] A. Lashab, D. Sera, J. M. Guerrero, L. Mathe, and A. Bouzid, "Discrete model predictive control-based maximum power point tracking for PV systems: overview and evaluation," *IEEE Transactions on Power Electronics*, vol. 33, no. 8, pp. 7272–7287, 2018.

[20] S. D. J. Mcarthur, E. M. Davidson, V. M. Catterson et al., "Multi-agent systems for power engineering applications—part II: technologies, standards, and tools for building multi-agent systems," *IEEE Transactions on Power Systems*, vol. 22, no. 4, pp. 1753–1759, 2007.

[21] R. Rahmani, I. Moser, and M. Seyedmahmoudian, "Multi-agent based operational cost and inconvenience optimization of PV-based microgrid," *Solar Energy*, vol. 150, pp. 177–191, 2017.

[22] F. Grabowski, "Nonextensive model of self-organizing systems," *Complexity*, vol. 18, no. 5, pp. 28–36, 2013.

[23] R. Hao, Q. Ai, Y. Zhu, and Y. Gao, "Cooperative optimal control of energy internet based on multi-agent consistency," *Automation of Electric Power Systems*, vol. 41, no. 15, pp. 10–17, 2017.

[24] M. Davison, C. L. Anderson, B. Marcus, and K. Anderson, "Development of a hybrid model for electrical power spot prices," *IEEE Power Engineering Review*, vol. 22, no. 3, p. 58, 2002.

[25] X. Yang, G. Wang, H. He, J. Lu, and Y. Zhang, "Automated demand response framework in elns: decentralized scheduling and smart contract," *IEEE Transactions on Systems, Man, and Cybernetics: Systems*, pp. 1–15, 2019.

[26] A. Ben-Tal and A. Nemirovski, "Robust convex optimization," *Mathematics of Operations Research*, vol. 23, no. 4, pp. 769–805, 1998.

[27] J. B. Rosen, "Existence and uniqueness of equilibrium points for concave n-person games," *Econometrica*, vol. 33, no. 3, pp. 520–534, 1965.

[28] M. N. Szilagyi and I. Somogyi, "Agent-based simulation of an n-person game with parabolic payoff functions," *Complexity*, vol. 15, no. 3, pp. 50–60, 2009.

[29] W. Saad, Z. Han, H. V. Poor, and T. Basar, "Game-theoretic methods for the smart grid: an overview of microgrid systems, demand-side management, and smart grid communications," *IEEE Signal Processing Magazine*, vol. 29, no. 5, pp. 86–105, 2012.

[30] G. Wang, W. Cai, Y. Zhang, K. Zhao, and X. Xu, "Lyapunov optimization based online energy flow control for multi-energy community microgrids," in *Proceedings of the 2019 IEEE PES GTD Grand International Conference and Exposition Asia (GTD Asia)*, Bangkok, Thailand, March 2019.